The synthesis of activated carbon electrode made from Acacia leaves (Acacia mangium wild) as a supercapacitors

by Agustino Agustino

Submission date: 08-Jul-2019 04:50PM (UTC+0700)
Submission ID: 1150103723
File name: from_Acacia_leaves_Acacia_mangium_wild_as_a_supercapacitors.docx (2.14M)
Word count: 3670
Character count: 19282

The synthesis of activated carbon electrode made from Acacia leaves (*Acacia mangium wild*) as a supercapacitors

E. Taer[1], K. Natalia[1], Apriwandi[1], R.Taslim[2], Agustino[1] and R. Farma[1]

[1]Department of Physics, University of Riau, 28293 Simpang Baru, Riau, Indonesia
[2]Departement of Industrial Engineering, State Islamic University of Sultan Syarif Kasim, 28293 Simpang Baru, Riau, Indonesia

Email: erman.taer@lecturer.unri.ac.id

Abstact. The activated carbon electrode made from acacia leaves (*Acacia mangium wild*) been developed successfully in 1 M H_2SO_4 electrolyte. The preparation carbon electrodes used a combination of chemical and physical activation with variation temperature of 800 °C, 850 °C, 900 °C and 950 °C. High specific capacitances of activated carbon as high as 113 F g^{-1} in two electrodes system exhibits excellent electrochemical performances. Additionally, activated carbon exhibits great purity carbon content as high as 95.73% with specific surface area of 714.492 m^2 g^{-1}. These excellent results show great potential in developing energy storage devices with high specific capacitance for supercapacitor application.

Keyword: acacia leaves; activated carbon; supercapacitor.

1. INTRODUCTION

Acacia (*Acacia mangium wild*) is one type of industrial tree plantations that was developed to be used as a support for various wood processing industries in Indonesia, one of which is the paper-making industry (pulp). High cellulose content and it grow quickly is the reason for the acacia tree to be the mainstay of pulp in the paper-making industry. However, not all parts of acacia trees are suitable to be pulped, for example leaves are only left to be neglected waste. Even though bark, wood and acacia leaves are alternative biomass reserves that have the potential to be developed as biosorbents [1, 2]. The component contained in acacia leaves are Tanin [3], saponins, cellulose and carbon with levels reaching 85.6% [1]. Utilization of acacia leaves has so far only been used as an absorbent medium. Therefore, in this study acacia leaf waste was used as a supercapacitor carbon electrode. The performance of the electrodes are determined by the surface area of the activated carbon formed. the surface area of high activated carbon will increase the number of absorbed ions to increase the specific capacitance of supercapacitors [4]. One way to expand the surface area of an electrode is through chemical and physical activation [5, 6, 7]. The process of preparation carbon electrodes from acacia leave waste in this study used a combination of chemical and physical activation. 0.5 M KOH was chosen as a chemical activation material and physical activation was carried out by flowing CO_2 gas at a temperature variation of 800 °C, 850 °C, 900 °C and 950 °C. It is hoped that the optimization of the preparation carbon electrodes from acacia leave waste is expected to have a cheap carbon source, high surface area and a high enough carbon content that will increase the performance of supercapacitors.

2. EXPERIMENTAL SECTION

2.1. Preparation activated carbon samples

The basic material is a type of biomass from acacia leaves. Acacia leaves were collected as 3 kg. The samples were pre-carbonized from a temperature of 50 ˚C to 200 ˚C for 2 hours. The pre-carbonized sample is milled and sieved to obtain a 53 µm particle size (Laboratory Test Sieve). 0.5 M KOH was chosen as a chemical activator. activated carbon powder changed into monolith without addition adhesive materials. The carbonization and physical activation carried out in one step process at N_2 and CO_2 gas amosphere [8, 9]. physical activaton temperature was varied of 800 ˚C, 850 ˚C, 900 ˚C and 950 ˚C. Finally monolith carbon that have been washed and dried are then polished to be are arranged in the sandwich form as supercapacitor cells [10].

2.2.Characterization of physical properties

Characterization of physical properties are commonly performed on carbon electrodes includes density expressed by a mass and volume unity, Scanning Electron Microscopy (SEM), X-ray Dispersive Energy (EDX), X-ray Diffraction (XRD) and Gas N_2 gas adsorption/desorption by using instrument of SUPRA S-3400N series, Philip X-Pert Pro PW 3060/10 with a source of Cu k-α rays, and Quantachrome Version 11.0, respectively.

2.3.*Characterization of electrochemical properties*

Cyclic Voltammetry (CV) is a popular method to analyzed capacitive properties of electrochemical cells. Cyclic Voltammetry (CV) were carried out by using CV UR Rad-Er 5841 instrument in 1 M H_2SO_4 electolyte and duck eggshells membrane as separator [11, 12] at the Material Physics and Nanotechnology Laboratory, Department of Physics, FMIPA, University of Riau .

3. DISCUSSION SECTION

3.1. Density analysis

The comparison of the average density of carbon electrodes before and after carbonization - activation shown in Figure 1. Figure 1 shows the electrode density has decreased after carbonization-physical activation. The density shrinkage for AcM800, AcM850, AcM900 and AcM950 is in the range of 32-38.5%. The decrease in the density of carbon electrodes due to the evaporation of non-carbon materials in the carbonization process and followed by the breakdown of the carbon chain from more complex compounds in the physical activation process. Evaporation of non-carbon material causes the pores widening and produce new pores in the electrode. Imperfect pores in the carbonization process will be rearranged in the physical activation process with relatively high temperatures. This phenomena causes depreciation density and increases the porosity properties of the sample.

In addition, the density influenced by the pellet forming process. Samples with the same mass do not necessarily produce the same density. The presence of sticky samples when pressing and the uneven surface of the pellets formed causes mass, thickness and diameter produced to be not exactly same so the density is not same. Carbon pellets that are feasible for carbonization-physical activation have several criteria including mass (0.62 g ≤mass≤

0.72 g), diameter (1.8 cm ≤diameter≤ 2.02 cm), thickness (0.21 cm ≤ thickness ≤ 0.3 cm) and density (0.72 g cm^{-3} ≤density≤ 1.12 g cm^{-3}). This difference in size will affect the optimization of the physical activation due to the different surface area so that it produces different electrode structures.

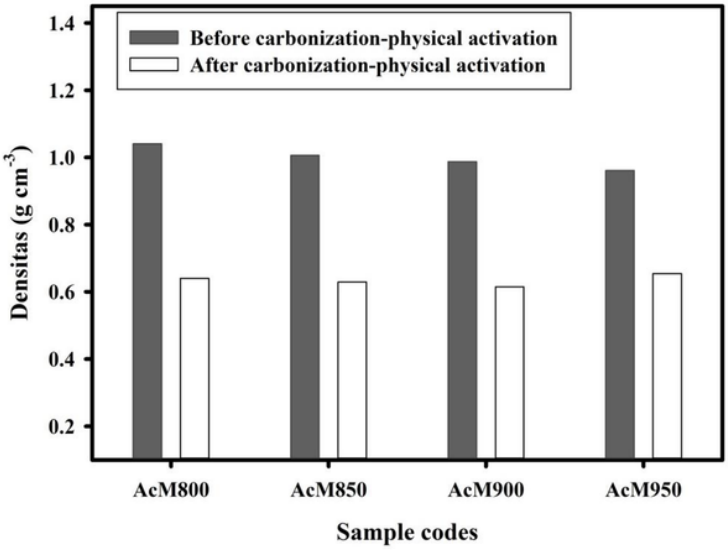

Figure 1. The density data in carbonization-physical activation effect

The density of carbon electrodes after carbonization-physical activation was decrease with increasing temperature except at a temperature of 950 ˚C. This indicates that at temperatures of 800 ˚C, 850 ˚C and 900 ˚C many impurities content are reduced and new pores are formed on carbon electrodes while at 950 ˚C there is a breakdown of carbon chains with non-carbon due to overheating so pores become damaged with more large pores [13] which caused the density for this sample to increase.

3.2. Thermogravymetry analysis

Thermogravimetric analysis (TGA) method used to analyze the thermal properties of a material as a function of increasing temperature. Figure 2 is a TGA profile consisting of Thermogravimetry (TG) and Differential Thermal Gravimetry (DTG). TG profile shows a mass decrease in persentage with increasing temperature. This decrease is caused by the mass decomposition of the material tested. TG profiles present three stages of mass decomposition. The first stage occurs at a temperature of 200.5 ˚C with a mass decomposition of 4.89%, indicated the water evaporation process. The second stage exhibits the greatest mass decomposition of 38.51% at a temperature of 351.6 ˚C. at this stage there are decomposition process of hemicellulose, cellulose and lignin. The third stage is the advanced decomposition stage of lignin [14] at a temperature of 550.7 ˚C. DTG curve shows the rate of weight lost in the sample. The maximum rate of weight lost as high as 0.154mg min^{-1} at a temperature of 335.7 ˚C. the temperature of 335.7 ˚C is the point where hemicellulose, cellulose and lignin decompose optimally. This analysis is supported by the TG profile which has drastically

decreased in range of same temperature. Based on TG and DTG profile analysis, it can be concluded that the temperature of 336.7 ˚C is thermal resistance from the acacia leaf powder for the next carbonization process. This thermal resistance is valid and acceptable because it is still in the range of thermal resistance for biomass materials such as ketapang leaves with a thermal resistance of 323.2 ˚C [15] and coconut leaves with a thermal resistance of 343 ˚C [16].

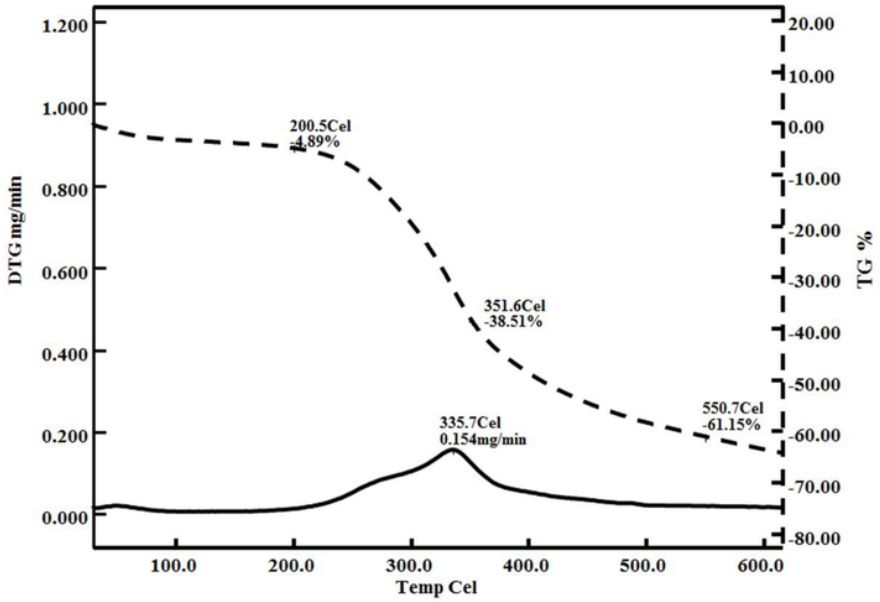

Figure 2. TG and DTG profiles for acacia leaves powder

3.3. Degree of cristallinity analysis

The X-Ray Diffraction (XRD) characterization aims to determine the degree of crystallinity of carbon electrode samples. Figure 3 is an XRD characterization pattern of carbon electrodes from acacia leaves. Figure 3 present two wide peaks with 2θ angles in the diffraction plane (002) and (100). The AcM800, AcM850, AcM900 and AcM950 samples exhibit 2θ angles in the diffraction plane (002) and (100) which correspond to carbon material from biomass as shown in table 1. These peaks look wide indicates an amorphous electrode structure [17, 18]. Calculations of lattice parameters such as layer height (L_c), layer width (L_a), and interlayer spacing (d_{hkl}) are obtained through the Microcal Origin software approach and it are calculated using standard Equations [19, 20, 21, 22], complete parameters $2\theta_{002}$, $2\theta_{100}$, d_{002}, d_{100}, L_c and L_a can be seen in Table 1.

Table 1. $2\theta_{002}$, $2\theta_{100}$, d_{002}, d_{100}, L_c and L_a parameters for Acs samples

Sample codes	$2\theta_{002}$ (°)	$2\theta_{100}$ (°)	d_{002} (Å)	d_{100} (Å)	L_c (Å)	L_a (Å)
AcM800	23,90	43,81	3,71	2,06	8,38	5,19
AcM850	23,51	44,84	3,77	2,01	8,37	17,29
AcM900	23,41	44,03	3,79	2,05	8,20	20,50
AcM950	22,82	44,14	3,89	2,04	6,98	9,15

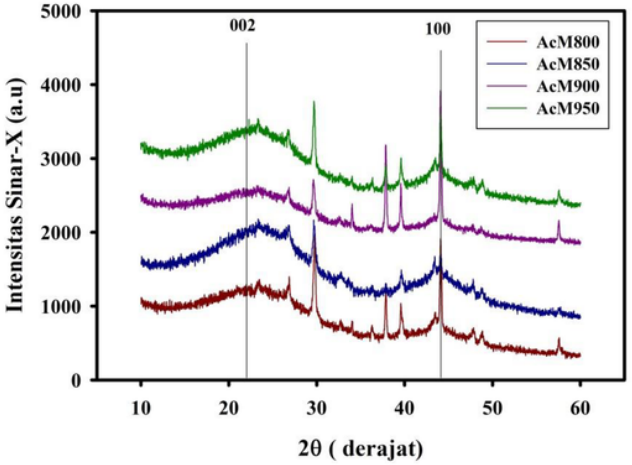

Figure 3. XRD pattern for AcM800, AcM850, AcM900 and AcM950 samples

The d_{002} interlayer spacing is shown to increase along with the increasing in physical activation temperature, while the d_{100} interlayer spacing shows irregularity. In another study it was also found that d100 did not experience regularity to activation temperature (ref). The L_c exhibit to decrease with increasing in physical activation tmperature, while the L_a does not show any regularity. The L_c can be used as a reference to determine the specific surface area. Based on the equation $S = 2/\rho L_c$ shows the L_c is inversely proportional to the surface area where, a small L_c will produce a large surface area [23, 24]. The higher surface area willl be support excelent specific capacitive.

3.4. Surface morphologycal analysis

SEM micrographs of carbon electrodes from acacia leaves (*Acacia mangium Wild*) are shown in Figure 4. SEM micrograph with a 5000 magnification present chunks of particles, pores between particles and carbon fibers. Figure 4.4a shows a large chunk of particle with a shiny surface and less visible pores on the surface of the particle. These particles exhibit also macro-sized pores and there are carbon fibers that spread almost evenly across the entire electrode surface. Figure 4.4b shows pores on the chunks of particle surface. Among these particles there are crack caused by continouing macro-sized pores and the carbon fibers seen relatively less than the sample AcM800. The AcM850 has a relatively larger number of pores with a relatively smaller pore diameter size compared with the AcM800, therefore it can be assumed higher temperature leads to larger mean pore size [25] and surface area of the AcM850 sample is higher than the AcM800. Figure 4.4c shows that chunks of particles with fine pores spread on the surface of the electrode. The relatively smaller pore diameter size indicates the surface area of the AcM900 electrode is greater than that of the AcM800 and AcM850. The clumps of carbon fiber on the surface appear to have a relatively higher density than the AcM850 electrode. Figure 4.4d shows most fine particle between all electrodes which indicates the AcM950 electrode has the smallest pore diameter size among all samples

therefore its the best porosity properties. The AcM950 has the least carbon fiber than all samples.

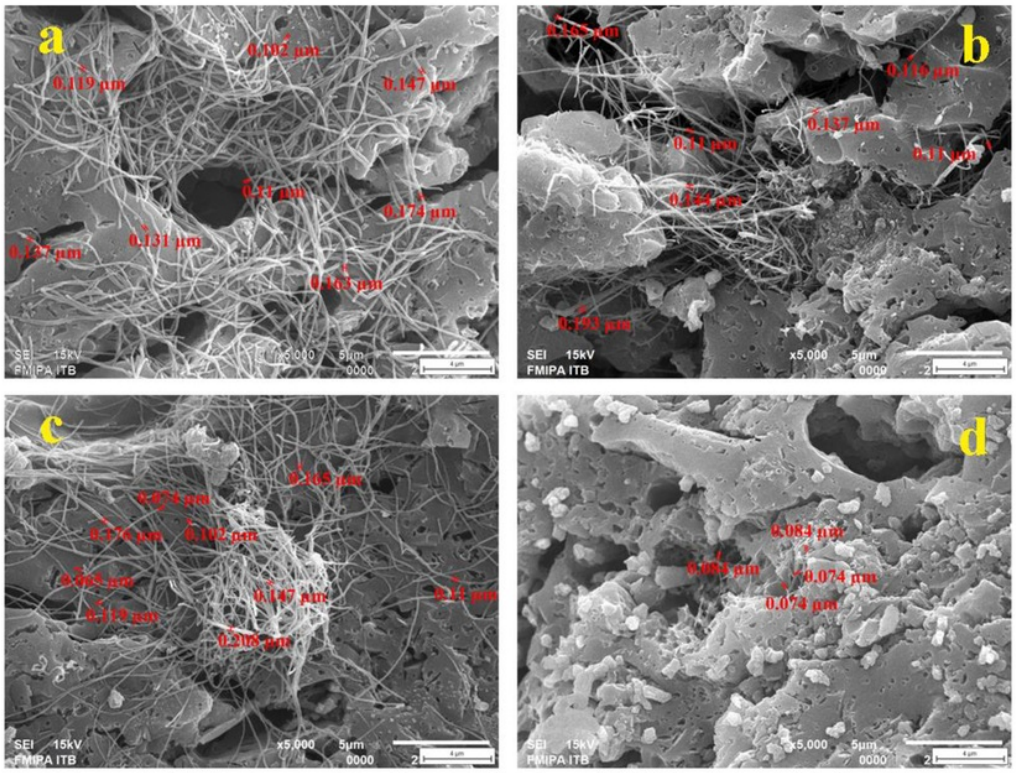

Figure 4. SEM micrographs with magnification of 5000 for a)AcM800; b)AcM850, c)AcM900; and d)AcM950 samples

The micrograph SEM with a 40000 magnification also present in Figure 4. The purpose of SEM characterization area selection is to examine further the shape and size of the fiber to the physical activation temperature. The form of carbon fiber produced resembles a tube, which can be call it the carbon nanotube structure. In more detail, it cannot be ascertained the existence of a hole along the fiber, but on the appearance of the fiber fracture shows the existence of cavities in the form of holes. In other studies the synthesis of carbon nano tubes from biomass materials has also been studied but requires additional special equipment (TEM) to ensure holes along the fiber [26].

Figure 5 shows the fiber's outer diameter varies with a range of 44.847-235.76 nm. The outer diameter of carbon fiber decreases with increasing physical activation temperature. The average outer diameter of 5 fibers measured for the AcM800, AcM850, AcM900 and AcM950 were 123.4618 nm, 104.8614 nm, 102.922 nm and 75.0598 nm respectively. The inner diameter of carbon fiber also decreases with the increase in physical activation temperature. The average inner diameter for the AcM800, AcM850 and AcM900 were 56.272 nm, 53.59 nm, and 25.144 nm. The inner diameter for the AcM950 electrode cannot be calculated due to limitations in the present of SEM data. The decreasing in outer and inner

diameters of the carbon fibers cause by erosion of the carbon fiber walls due the high physical activation temperatures.

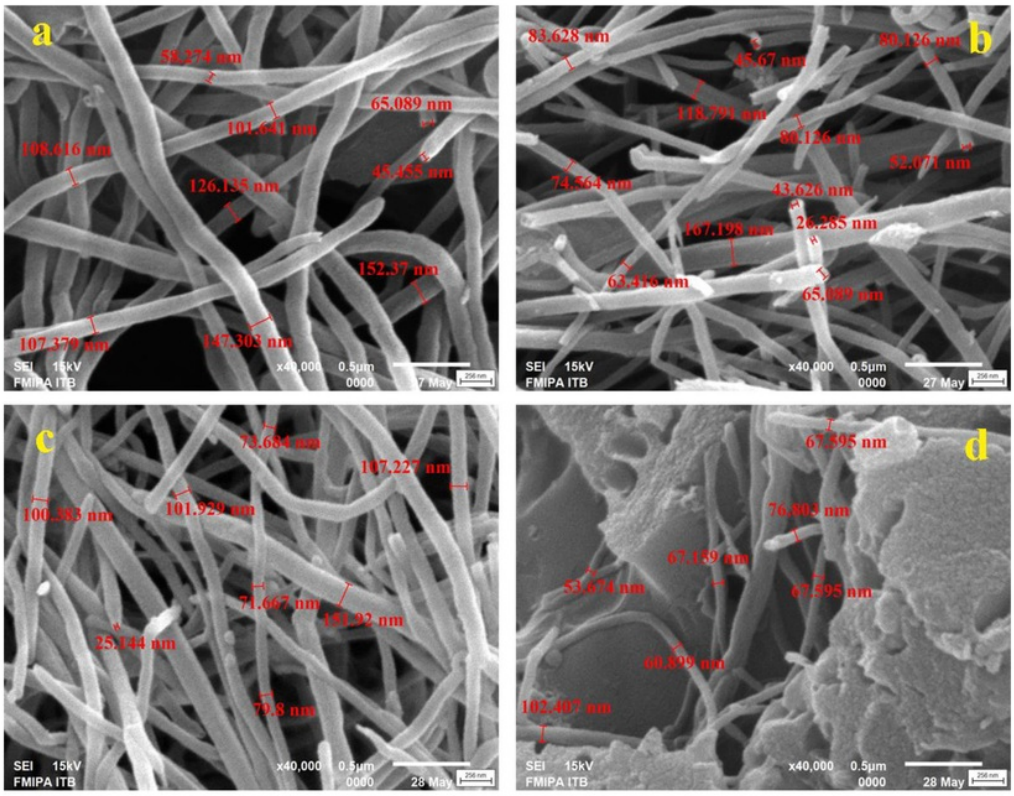

Figure 5. SEM micrographs with magnification of 40000 for a)AcM800; b)AcM850, c)AcM900; and d)AcM950 samples

3.5. Chemical content analysis

Energy Dispersive X-Ray (EDX) characterization aims to determine the chemical composition contained in activated carbon electrode samples. The results of the EDX characterization of carbon electrodes found the high carbon (C) content. Other elements obtained are oxygen (O), magnesium (Mg), silica (Si), potassium (K), and calcium (Ca). The percentage of the elemental content can be seen in Table 2.

The types of elements contained in the electrode decrease with increasing physical activation temperature, indicates that the more pure carbon produced due to the evaporation of other elements than carbon along with the increased physical activation temperature. The evaporating elements include magnesium (Mg) and potassium (K) at a temperature of 900 ˚C and silica (Si) at a temperature of 950 ˚C. The other elements content than carbon is caused by the basic element content of acacia leaves such as calcium and magnesium [27]. The effect of samples preparing in the study also affects the other elements content such as silica due to the initial washing process which is not too clean which causes the content of sand composed of silica, and potassium (K), oxygen (O) due to chemical activation by using KOH. Carbon

content for all variations in activation temperature shows irregularities. Carbon content for AcM800, AcM850, AcM900 and AcM950 were 94.49%, 92.62%, 95.75% and 91.16% respectively. This change in carbon content is clearly influenced by the elemental content of oxygen (O) where the oxygen content for AcM800, AcM850, AcM900 and AcM950 are 2.26%, 4.57%, 2.76%, and 6.39 % respectively.

Table 2. Chemical contents for Acs electrode samples

Element	Sample codes			
	AcM800 (%)	AcM850 (%)	AcM900 (%)	AcM950 (%)
Karbon (C)	94,49	92,62	95,73	91,16
Oksigen (O)	2,26	4,57	2,76	6,39
Magnesium (Mg)	0,22	0,23		
Silika (Si)	0,13	0,32	0,37	
Kalium (K)	0,63	0,35		
Kalsium (Ca)	2,26	1,92	1,14	2,45
Totals	100%			

3.6. N_2 gas adsorption/desorption analysis

N_2 gas absorption characterization using the Brauner-Emmet-Teller (BET) method aims to determine the specific surface area and the pore characteristics of the carbon electrodes. Figure 6 shows N_2 gas absorption with a IV type based on IUPAC calsification. The IV type curve shows an increase in absorption at low pressure and there is a hysteresis loop that indicates the carbon sample has pores with micro and meso sizes which are predominantly mesoporous [28]. This corresponds to Figure 7 where the pore diameter size distribution for acacia leaf electrodes is in the range of 2-20 nm with the average pore ranges of 3.1-3.2 nm. BET surface area of AcM800, AcM850, AcM900 and AcM950 are 631.523 $m^2\ g^{-1}$, 675.539 $m^2\ g^{-1}$, 687.516 $m^2\ g^{-1}$, and 714.492 $m^2\ g^{-1}$ respectively, forethemore it can be concluded the surface area increases to the physical activation temperature.

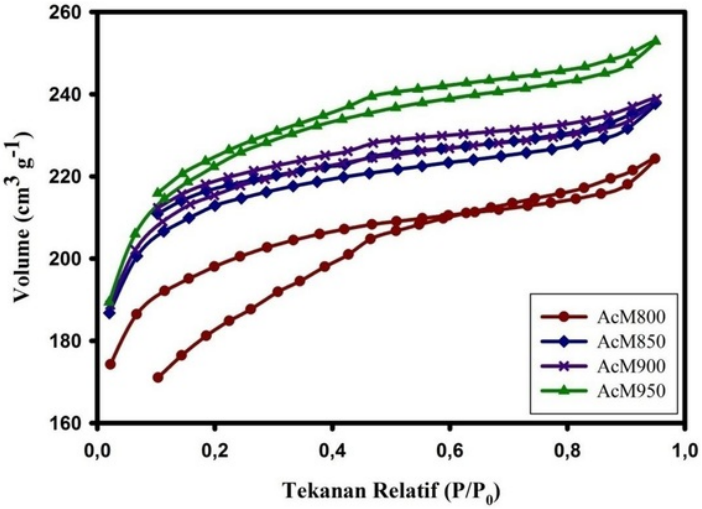

Gambar 6. N_2 gas adsorption/desorption for all samples

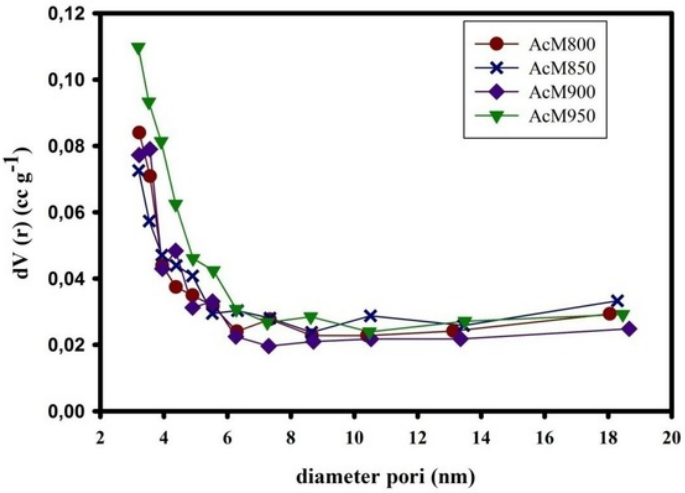

Gambar 7. Distribution pores of activated carbon electrode from acacia leaves

3.7. The specific capasitive analysis

Cyclic Voltammetry (CV) method aims to determine the specific capacitance of supercapacitor cells. The CV curve is rectangular which contains the charging current (charge) and discharge flow (discharge) to the potential window (V). The shape of the curve depends on the charge and discharge current. The greater charge and discharge current, the wider shape of the curve indicates the greater of specific capacitance [29, 30]. The charge current is a measured when ions filling process into the electrode pores labeled by the upper curve and the otherside when ions go out of electrode pores called discharge current which labeled by a lower curve. The results of CV measurements shown in Figure 8.

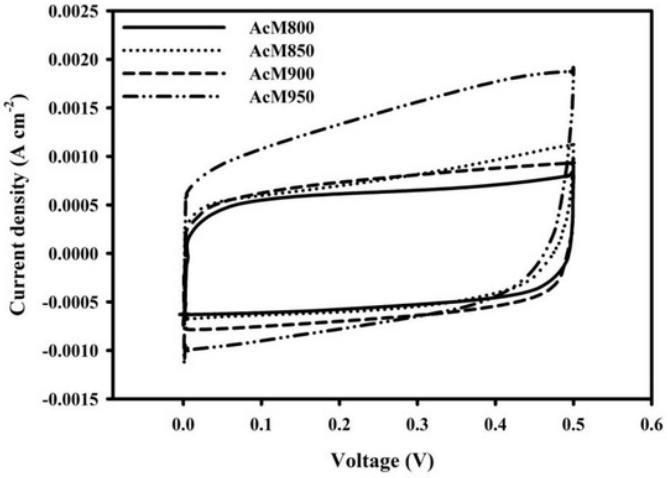

Figure 8. CV curve for Acs samples

Table 3. The specific capacitances for Acs samples

Sample codes	Scan rate ($V\ s^{-1}$)	Mass (g)	I_c (A)	I_d (A)	C_{sp} ($F\ g^{-1}$)
AcM800	0,001	0,015	0,000638	-0,00054	78
AcM850	0,001	0,01645	0,000745	-0,00058	80
AcM900	0,001	0,0128	0,000728	-0,00059	102
AcM950	0,001	0,01615	0,00146	-0,00038	113

Based on Figure 8, the current increases with increasing physical activation temperature. The largest to the smallest curves is found by the cells of AcM950, AcM900, AcM850 and AcM800. The width of the charge and discharge current curves also corresponds to the specific capacitance. The specific capacitance calculated by using standard equation and for each samples presented in Table 3. Based on the Table 3 an increasing in physical activation temperature causes an increasing in specific capacitance, where from AcM800 to AcM950 samples the specific capacitance has increased from 78 F g^{-1} to 113 F g^{-1}.

Overall, there is a relationship between specific capacitance by physical variables such as surface morphology, layer height, and BET surface area. The higher physical activation temperature cause the smaller of particle size and layer height, and higher surface area. All of these variables support the increasing in the specific capacitance.

4. CONCLUSSION

High specific capacittance of activated carbon electrodes is synthesized from dry waste in the form of acacia leaves without addition adhesive materials and studied for supercapacitor application. Activated carbon synthesized at various of physical activation temperature of 800 °C, 850 °C, 900 °C and 950 °C present specific capacitance of 78 F g^{-1}, 80 F g^{-1}, 102 F g^{-1} and 113 F g^{-1}, respectively. This high supercapacitor performance supported by density, degree of cristallinity, chemical content and specific surface area. The density of carbon electrodes was decrease with increasing temperature. surface morphologycal electrode exhibit carbon fibers in range diameter of 25.144-235.76 nm. The surface area increases to the physical activation temperature of 631.523 m2 g-1, 675.539 m^2 g^{-1}, 687.516 m^2 g^{-1}, and 714.492 m^2 $g^{-1}$for AcM800, AcM850, AcM900 and AcM950 samples respectively.

ACKNOWLEDGEMENTS

The author would like to thank the DRPM Kemenristek-Dikti through the third year Project of PDUPT with the title "Potential of Urban Solid Waste Utilization as a Supercapacitor Electrode" with contract number: 759/UN.19.5.1.3/PT.01.03/2019.

References

1. F. Hasfita, *J. Teknologi Kimia Unimal* 1 (2002) 36.
2. A. Nurkaromah, Sukandar, *J. Env. Engineering & Waste Managemen,* 2 (2017) 79.
3. S. A. Abdulrazaka, T. Fujiharaa, J. K. Ondiek , E. R. Érskov, *Animal Feed Science and Technology*, 85 (2000) 89.
4. Z. A. Zhang, M. Cui, Y. Q. Lai, J. Li Y. X. Liu, *J. Central South University of Technol.,* 16 (2009) 0091.
5. C. O. Ania, J. Pernak, F. Stefaniak, E. Raymundo-Pinero, F. Bequin, *Carbon,* 47 (2009) 3158.
6. S. Guo, Jia, Lua, A. Chong, *Carbon*, 38 (2000) 19853.
7. Z. S. Iro, C. Subramani, S. S. Dash, *Int. J. Electrochem. Sci.,* 11 (2016) 10628.
8. E. Taer, Apriwandi, Yusriwandi, W. S. Mustika, Zulkifli, R. Taslim, Sugianto, B. Kurniasih, Agustino, P. Dewi, *AIP Conf. Proc.*, 1927 (2018) 030036-1.
9. E. Taer, A. Apriwandi, R. Taslim, U. Malik, Z. Usman, *Int. J. Electrochem. Sci.,* 14 (2019) 1318.
10. E. Taer, R. Taslim, W. S. Mustika, B. Kurniasih, Agustino, A. Afrianda, Apriwandi, *Int. J. Electrochem. Sci.,* 13 (2018) 8428.
11. E. Taer, R. Taslim, *AIP Conf. Proc.,* 1927 (2018) 020004-1.
12. E. Taer, Sugianto, M. A. Sumantre, R. Taslim, Iwantono, D. Dahlan, M. Deraman, *Adv. Mater. Research,* 896 (2014) 66.
13. R. Satish, V. Aravin, W. C. Ling, N. K. Woei, S. Madhavi, *Electrochimica Acta*, 182 (2015) 478.
14. M. Brebu, C. Vasile, *Cellulose Chemistry Technology,* 49 (2010) 353.
15. E. Taer, A. Afrianda, R. Taslim, Krisman, Minarni, A. Agustino, U. Malik, A. Apriwandi, *J. Phys.: Conf. Ser.,* 1120 (2018) 012007.
16. K. S. Sulaiman, A. Mat, A. K. Arof, *Ionics,* 22 (2015) 911.
17. W. Cao, F. Yang, *Mater. Today Energy*, 9 (2018) 406.
18. G. Yu, L. Lei, J. Yuming, W. Yu, Y. Chuanjun, W. Yingjin, C. Gang, G. Junjie, L. Haiyan, *Appl. Energy,* 153 (2015) 41.
19. B. D. Cullity, Elements of X-Ray Diffraction, Ed. 3, (2001) Amazon Prentice Hall.
20. P. J. M. Carrott, J. M. V. Nabais, M. M. L. R. Carrott, J. A. Pajares, *Carbon,* 39 (2001) 1543.
21. J. M. V. Nabais, J. G. Teixeira, I. Almeida, *Bioresource Technol.,* 102 (2010) 2781.
22. F. Li, W. Chi, Z. Shen, Y. Wu, Y. Liu, H. Liu, *Fuel Process Technol.,* 91 (2010) 17.
23. K. Kumar, R. K. Saxena, R. D. Kothari, K. Suri, N. K. Kaushik, J. N. Bohra, J. N, *Carbon,* 35 (1997) 1842.
24. M. Deraman, R. Daik, S. Soltaninejad, N. S. M. Nor, Awitdrus, R. Farma, N. F. Mamat, N. H. Basri, M. A. R. Othman, *Adv. Mater. Research,* 1108 (2015) 1.
25. P. Simon, Y. Gogotsi, *Nature Mater.*, 7 (2008) 845.
26. N. Tripathi, V. Pavelyev, S. S. Islam, *Appl Nanosci.,* 7 (2017) 557.
27. Djarwanto, S. Suprapti, R. A. Pasaribu, *Jurnal Penelitian Hasil Hutan,* 27 (2009) 303.
28. S. K. Sing, H. D. Everett, W. A. R. Haul, L. Moscou, A. R. Pierotti, J. Rouquerol, T. Siemieniewska, *Pure & App. Chem.,* 57 (1985) 603.
29. E. J. Ra, E. Raymundo-Piñero, Y. H. Lee, F. Béguin, *Carbon,* 47 (2009) 84.
30. B. Armynah, E. Taer, Z. Djafar, W. H. Piarah, D. Tahir, *Int. J. Electrochem. Sci.,* 14 (2019) 7076.

The synthesis of activated carbon electrode made from Acacia leaves (Acacia mangium wild) as a supercapacitors

ORIGINALITY REPORT

4%	0%	4%	%
SIMILARITY INDEX	INTERNET SOURCES	PUBLICATIONS	STUDENT PAPERS

PRIMARY SOURCES

1	E Taer, R Radiawan, R Taslim, Awitdrus, A Apriwandi, Krisman, Minarni, A Agustino, R Farma, R N Setiadi. "The effect of microwave irradiation in activated carbon processing from sago waste to physical and electrochemical properties of electrode supercapacitor cells", Journal of Physics: Conference Series, 2018 Publication	4%

Exclude quotes	On	Exclude matches	< 2%
Exclude bibliography	On		